Proceedings of PVP2008
2008 ASME Pressure Vessels and Piping Division Conference
July 27-31, 2008, Chicago, Illinois, USA

PVP2008-61513

NUMERICAL INVESTIGATION TO EXAMINE THE EFFECT OF INTRODUCING A CRACK IN A RESIDUAL STRESS FIELD

Simon Kamel
Dept. of Mechanical Engineering
Imperial College London
South Kensington Campus
London SW7 2AZ
UK
s.kamel@imperial.ac.uk

Noel P. O'Dowd
Dept. of Mechanical and
Aeronautical Engineering
Materials and Surface Science Institute
University of Limerick
Limerick, Ireland
noel.odowd@ul.ie

Kamran M. Nikbin
Dept. of Mechanical Engineering
Imperial College London
South Kensington Campus
London SW7 2AZ
UK
k.nikbin@imperial.ac.uk

ABSTRACT

This paper presents a detailed two dimensional finite-element study to examine the effect of introducing a crack either progressively or instantaneously into a residual stress field. A progressive crack is defined as a crack which is introduced in fixed increments of crack extension until the desired crack length is achieved. An instantaneous crack is one in which a crack of the required length is introduced instantaneously into the finite-element mesh. Inspection is made of the crack tip fields and the crack opening displacements. A modified definition of the J-integral, which accounts for the initial plastic strain due to residual stress, is assessed, in order to examine its ability to characterise the intensity of the near crack tip fields. The implications of the results on fracture assessment of structural components are discussed.

INTRODUCTION

In components containing cracks, the presence of residual stress, e.g. due to welding, can have a detrimental effect on structural integrity, and it is therefore important to include the contribution of such stress in a fracture assessment. Procedures such as R6 [1] take no account of the prior history of crack formation on the crack driving force. Such an assumption may give overly conservative predictions of the integrity of a component. Although studies have been performed to examine the effect of a growing crack in a primary stress field (e.g. [2] and [3]), studies of a growing crack in a residual stress field are limited. In [4], a finite-element study was carried out in which simultaneous and progressive cracks were introduced in a residual stress field in a 3D notched compact tension geometry. The crack tip fields for the progressive and simultaneous cracks were found to be in close agreement at the mid-plane and the surface of the geometry. It was also shown that the crack opening displacement and the crack driving force (J-integral) were always lower for a progressive crack analysis.

A similar approach to that taken in [4] is adopted in this work. We focus here on a finite-element investigation of a 2D specimen under plane strain and plane stress conditions to examine the effect of the history of crack formation on the crack driving force due to residual stress. Following the notation in [4] we consider the introduction of a 'simultaneous' and a 'progressive' crack in a residual stress field. A 'progressive' crack is one which is introduced in fixed increments of crack extension until the required crack length is achieved, whereas a 'simultaneous' crack is one in which a crack of the required length is introduced instantaneously. The crack tip fields and the crack face displacements are compared to examine whether they are affected by the method of crack introduction. A modified definition of J-integral, which allows for the initial plastic strain due to residual stress, is assessed to examine its ability to characterise the intensity of the crack tip fields. We consider the effect of

mesh resolution along the crack flank on the results.

CALCULATION OF J IN THE PRESENCE OF A RESIDUAL STRESS FIELD

A modified definition of J which accounts for the presence of residual stress was introduced in [5] as,

$$J = \int_{\Gamma} \left(W\delta_{1i} - \sigma_{ij} \frac{\partial u_j}{\partial x_1} \right) n_i ds + \int_A \left(\sigma_{ij} \frac{\partial \varepsilon^0_{ij}}{\partial x_1} \right) dA \qquad (1)$$

where ε^0_{ij} is an initial strain which arises due to elastic incompatibility of different parts of the structure. This can be for example, a thermal strain or a plastic strain due to residual stress in the structure. In Eq. 1, A is the area enclosed by the contour, Γ, and W the mechanical strain energy density, defined as,

$$W = \int_0^{\varepsilon^m_{ij}} \sigma_{ij} d\varepsilon^m_{ij} \qquad (2)$$

where ε_m is the mechanical strain which is related to the stress through the constitutive law. An additional modification to J has been proposed in [6] to account for the effect of non-proportional loading on the path dependence of J. This additional term has not been included in the current analysis, but will be considered in future work.

Commercial finite-element packages such as ABAQUS [7] have the capability to calculate J when ε^0_{ij} is a thermal strain but not for the case of an initial plastic strain due to residual stress. An independent post-processor, [5], has therefore been used which calculates J in accordance with eq. 1 using results from an ABAQUS analysis.

FINITE ELEMENT PROCEDURES

In this investigation, we consider a plane 2D specimen. Initially the specimen is loaded under four point bending, as shown schematically in Fig. 1. Subsequently, the load is removed, leading to a residual stress distribution in the specimen. A crack of length $a/w = 0.2$, where a is crack length and w is specimen width, is then introduced, either instantaneously or progressively.

Finite element mesh

A typical finite-element mesh is shown in Figure 2. Symmetry allows for half the geometry to be modelled. The geometry is modelled using square and rectangular elements, with increased mesh resolution close to the crack tip. The crack tip is located at position $y = 0$, $x = 0.2w$.

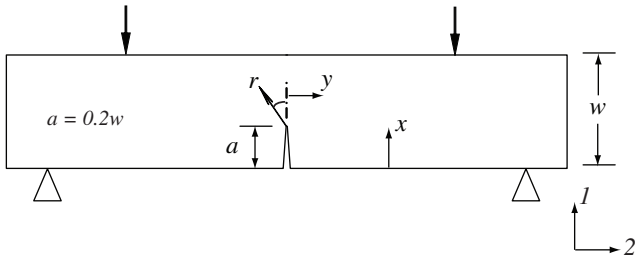

Figure 1. SCHEMATIC OF CRACKED GEOMETRY

For the progressive crack, the crack length is increased incrementally by releasing nodes along the crack flank. Finite-element analyses which involve node-release or element removal are generally expected to show some mesh sensitivity. Analysis has therefore been carried out for four cases of increasing mesh resolution along the crack flank as follows:

Case 1: uniform width elements of $a/250$ along crack flank
Case 2: uniform width elements of $a/500$ along crack flank
Case 3: uniform width elements of $a/250$ for $x < 0.8a$ and $a/1500$ for $0.8a < x < 1.0a$
Case 4: uniform width elements of $a/400$ for $x < 0.99a$ and $a/10,000$ for $0.99a < x < 1.0a$

Figure 2 shows the finite-element mesh for the analysis designated Case 4. Only the mesh in the region of the crack tip is shown. The elements ahead of the crack tip ($x > a$) are biased towards the crack tip to give a crack tip element width of approx. $10^{-5}a$. A sharp crack is modelled, with a single node at the crack tip. Analysis is performed for each mesh for a simultaneous crack and a progressive crack.

The finite-element analyses were performed using ABAQUS 6.6. Four-noded two dimensional plane strain or plane stress elements have been used. For the plane strain analysis, 'hybrid' elements have been used (ABAQUS element type CPE4H) to avoid any numerical difficulties associated with incompressible plasticity; for the plane stress analysis, standard plane stress elements have been used (ABAQUS element type CPS4). The analysis used a small displacement formulation.

Material Response

The stress-strain response assumes isotropic hardening and has the following form,

$$\begin{aligned} \frac{\varepsilon}{\varepsilon_0} &= \frac{\sigma}{\sigma_0} && \text{for } \sigma \le \sigma_0 \\ \frac{\varepsilon}{\varepsilon_0} &= \left(\frac{\sigma}{\sigma_0} \right)^n && \text{for } \sigma > \sigma_0 \end{aligned} \qquad (3)$$

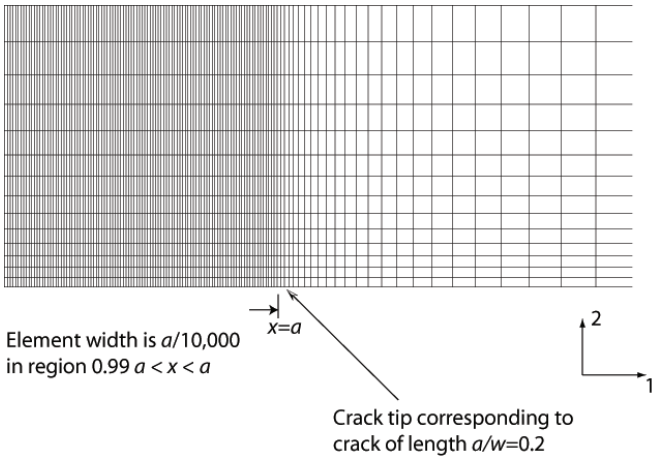

Figure 2. FINITE ELEMENT MESH (CASE 4) IN THE REGION OF THE CRACK OF LENGTH $a/w = 0.2$

where n is the strain hardening exponent, σ_0 is a normalising stress which is usually related to the yield stress and $\varepsilon_0 = \sigma_0/E$ where E is the Young's Modulus. In this study, analyses have been performed for n of 5 and 10 and σ_0/E of 500, representative of typical engineering steels. The material model is implemented using an incremental plasticity model. The material unloads elastically along the original elastic line without hysteresis.

Introduction of residual stress field

The residual stress is introduced into the uncracked body by applying a load to deform the geometry plastically. On removal of this load, a residual stress remains in the uncracked body, due to the presence of non-uniform plastic strains. The same load is applied for the plane strain and plane stress analyses. The magnitude of the load was chosen to give a moment along the symmetry line ($y = 0$) of $1.1M_0$, where M_0 is the plane strain limit moment of the un-cracked body, defined as,

$$M_0 = \frac{2}{\sqrt{3}} \frac{w^2}{4} \sigma_0 \tag{4}$$

The crack is subsequently introduced by releasing nodes along the symmetry line until the required crack length, $a/w = 0.2$, is achieved. The nodes are released by redefining the boundary conditions to remove the boundary constraints from those nodes. For the instantaneous crack, all the nodes on the crack face are released simultaneously. This is designated below as a 'simultaneous crack'. Alternatively, in the analysis designated as a 'progressive crack', the crack is introduced by releasing the nodes sequentially, i.e. one node per analysis step, followed by

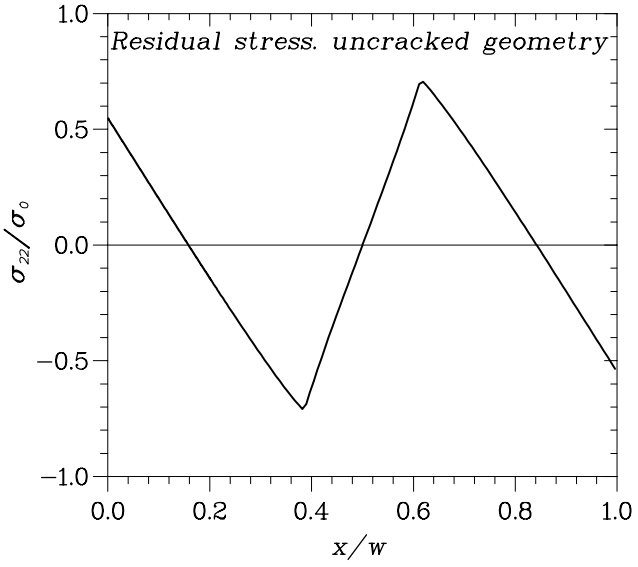

Figure 3. RESIDUAL STRESS (σ_{22}) DISTRIBUTION ALONG THE SYMMETRY LINE ($y = 0$) IN THE UNCRACKED GEOMETRY, FOR $n = 10$ AND PLANE STRAIN CONDITIONS

a static equilibrium analysis, until a crack length of $a/w = 0.2$ is achieved. For example, for Case 2, this corresponds to increments of crack extension of $a/500$ per analysis step.

RESULTS

Normal σ_{22} stress distributions

Figure 3 shows the residual stress distribution in the uncracked specimen along the symmetry line ($y = 0$) for $n = 10$ and plane strain. The residual stress distribution may be seen to be self-balancing (resultant force and moment is zero) and is tensile on the face on which the crack will be introduced. Note that the stresses plotted here and in all subsequent plots of stress (and strain) are evaluated at the centroid of the element. The uncracked residual stress profile for plane stress and for $n = 5$ is similar to Fig. 3, though the magnitude of the stress is slightly different.

In Fig. 4, the stress distributions following introduction of the crack of length $a/w = 0.2$ are presented. Distributions of normal (σ_{22}) stress ahead of the crack tip ($x > a$) are provided for a material with $n = 10$ under plane strain conditions. The results for the simultaneous and progressive crack analyses are presented in Figs. 4(a) and 4(b), respectively for the mesh Cases 1 to 4 described above. It may be seen that the mesh resolution along the crack flank in the region of the crack tip has a significant effect on the crack tip stresses, particularly for the progressive crack case. However, the distributions for Cases 3 and 4, for which the crack tip element width behind the crack tip are

$a/1500$ and $a/10,000$, respectively, lie close to each other. Thus the stresses appear to converge with increasing mesh refinement, for both the progressive and simultaneous crack analyses.

The normal (σ_{22}) stress distributions for simultaneous and progressive cracks are compared in Figs. 5(a) and 5(b) for plane strain and plane stress conditions, respectively, for mesh Case 4. It may be seen that for both cases the near tip stress is slightly higher for the simultaneous crack analysis, though for the plane strain case, the stress for the progressive crack analysis is higher at distances further from the crack tip.

Similar trends have been observed for $n = 5$—for brevity the results are not shown here.

Equivalent plastic strain distributions

Figure 6 shows the distributions of equivalent plastic strain ahead of the crack tip for plane strain and plane stress conditions for the Case 4 mesh (considered to be the converged solution). For plane strain conditions (Fig. 6a), the plastic strain distributions from the simultaneous and progressive crack analyses are similar except very close to the crack tip where the plastic strain is more than twice that from the progressive crack analysis. For plane stress conditions (Fig. 6b), the plastic strains from the simultaneous crack analysis are higher over a larger distance ahead of the crack tip. Note that in all cases examined the higher plastic strain (and stress) field are predicted for the 'simultaneous' crack analysis.

Figure 7 gives the distributions of equivalent plastic strain along the crack flank ($x < a$) after the crack has been introduced. It is clear for the progressive crack analysis, that a significant plastic wake is generated as the crack is introduced progressively into the finite-element mesh. The plastic strains along the crack flank are significantly lower for the simultaneous crack analysis. Note that for the simultaneous crack analysis, the majority of the plastic strain generated along the crack flank was introduced by the mechanical deformation, i.e. the additional plastic strain along the crack flank generated by introduction of the 'simultaneous crack' is negligible. This is not the case for the progressive crack analysis. As the crack is progressively introduced, a plastic zone is generated ahead of the newly introduced 'progressive' crack leading to the resultant plastic wake behind the final crack tip position.

It should also be noted (though not shown here) that the magnitude of the plastic strain in the crack wake is mesh dependent, with the magnitude of plastic strain increasing with increasing mesh density in the crack flank region. Similar behaviour is observed for the plane stress case, though the plastic strain are larger (consistent with Fig. 6).

Crack face displacements

The crack face vertical displacements (crack opening displacement) are compared in Fig. 8 for the progressive and simultaneous crack analyses. The results shown are from a plane strain analysis (the same trends were observed under plane stress conditions). Similar opening displacements are obtained for the two cases, with the values obtained from the simultaneous crack analysis somewhat higher than those from the progressive crack analysis. It may be noted that there is a rather abrupt change in slope of the displacement very close to the crack tip for the si-

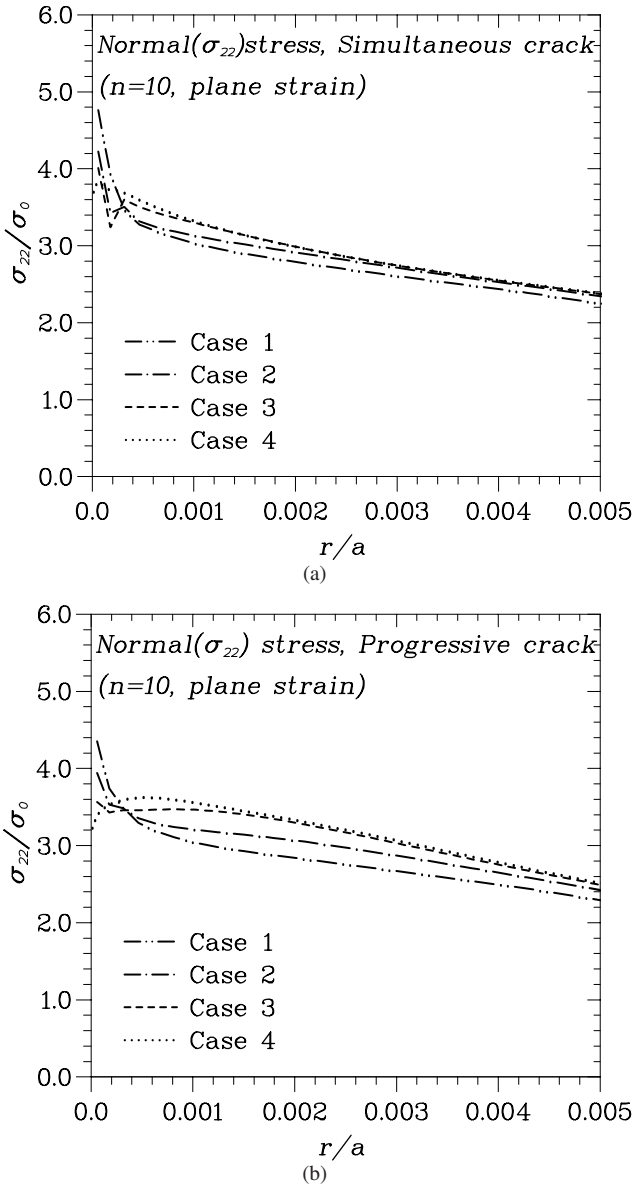

Figure 4. NORMAL RESIDUAL STRESS (σ_{22}/σ_0) DISTRIBUTIONS AHEAD OF THE CRACK OF LENGTH $a/w = 0.2$ ALONG THE SYMMETRY LINE ($y = 0$), FOR $n = 10$ AND PLANE STRAIN FOR (a) SIMULTANEOUS and (b) PROGRESSIVE CRACK

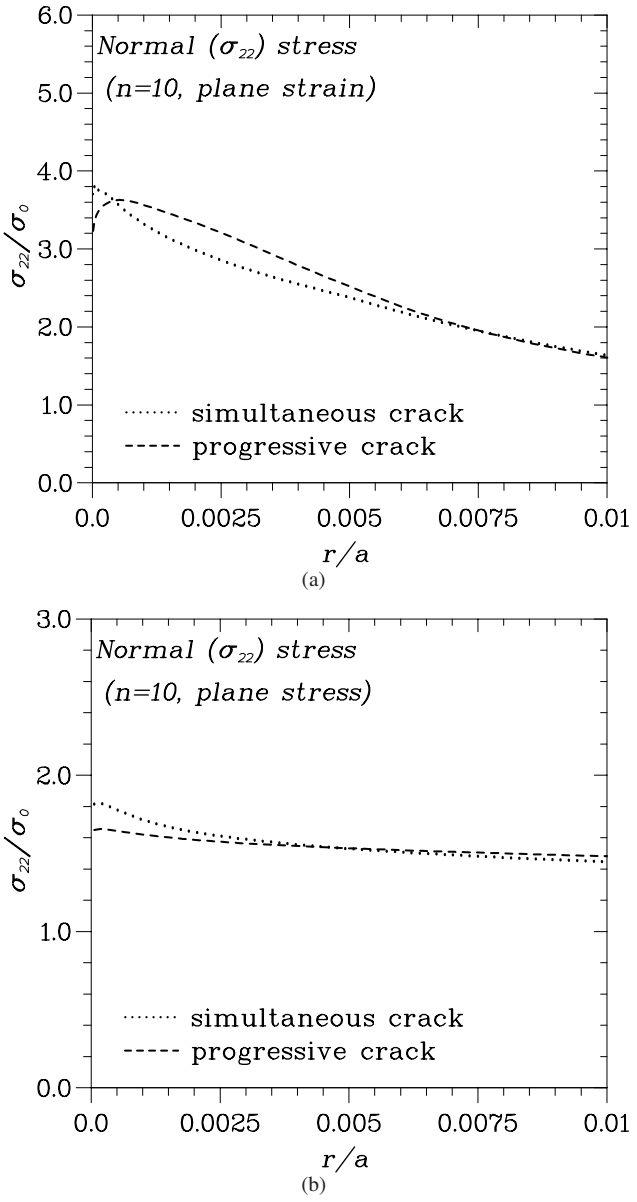

Figure 5. NORMAL RESIDUAL STRESS (σ_{22}/σ_0) DISTRIBUTIONS AHEAD OF THE CRACK OF LENGTH $a/w = 0.2$ ALONG THE SYMMETRY LINE ($y = 0$), FOR $n = 10$ AND (a) PLANE STRAIN, (b) PLANE STRESS CONDITIONS

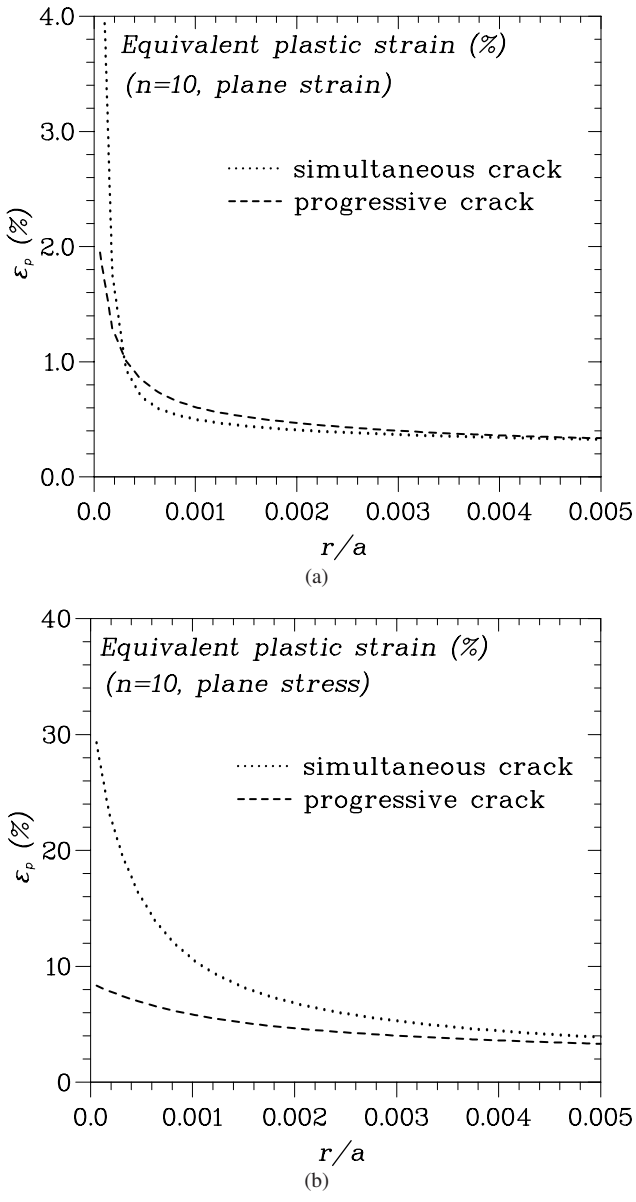

Figure 6. EQUIVALENT PLASTIC STRAIN (%) DISTRIBUTIONS AHEAD OF THE CRACK OF LENGTH $a/w = 0.2$ ALONG SYMMETRY LINE ($y = 0$) FOR $n = 10$ AND (a) PLANE STRAIN, (b) PLANE STRESS CONDITIONS. BOTH ANALYSES ARE FOR MESH CASE 4.

multaneous crack analysis. This is believed to be an artifact of the mesh design and is associated with the first few nodes behind the final crack tip position. The same trend in the crack opening displacement behaviour has been observed in [4], with the displacements at the mid-plane of a 3D specimen from a simultaneous crack analysis up to 20% higher than those from a progressive crack analysis.

Results for J-integral

We next consider the results for the J-integral for the simultaneous and progressive crack analyses. In Fig. 9, J given by eq. 1 (designated in the figure as 'Modified J') is compared with J calculated by ABAQUS for the simultaneous crack analysis using mesh Case 4 for the first 40 domains. It may be seen that the modified J definition gives reasonable path independence for all

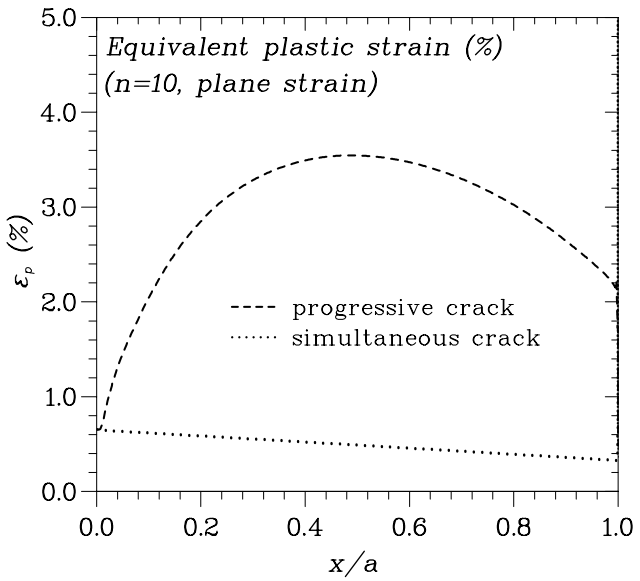

Figure 7. EQUIVALENT PLASTIC STRAIN ALONG THE CRACK FACE FOR THE CRACK OF LENGTH $a/w = 0.2$, FOR $n = 10$ AND PLANE STRAIN. BOTH ANALYSES ARE FOR MESH CASE 4.

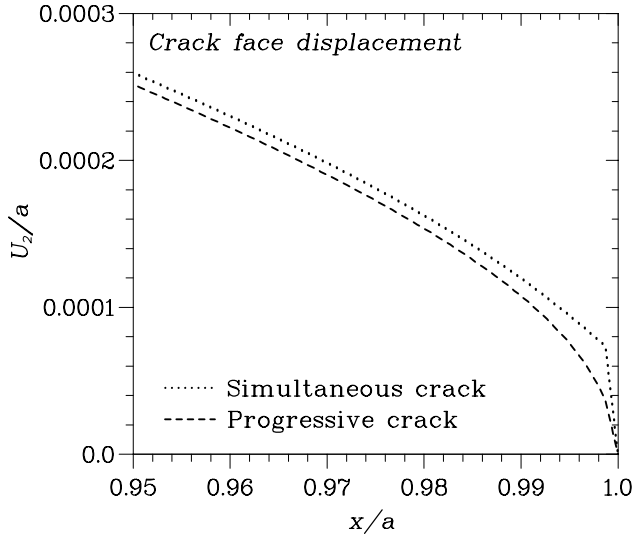

Figure 8. CRACK FACE OPENING DISPLACEMENT (U_2/a) ALONG THE CRACK FLANK FOR THE CRACK OF LENGTH $a/w = 0.2$, FOR $n = 10$ AND PLANE STRAIN

domains. The ABAQUS J is almost coincident with the modified J up to about the 20th domain, after which path dependence is observed. For the simultaneous crack analysis, the J value is relatively mesh insensitive for the four meshes analysed. The J value from the simultaneous crack analysis is compared with that from the progressive crack analysis for the four mesh cases in Fig. 10. Somewhat surprisingly (in view of the elastic unloading in the crack wake) the J values from the progressive crack analysis remain reasonably path independent. However, it may be seen that for the progressive crack analysis, J reduces with increasing mesh refinement behind the crack tip and appears to approach zero. It is noted that in [3], in which a finite-element analysis was performed for limited growth of a pre-existing crack, that the J value approaches zero as the contour surrounding the crack tip is shrunk to the crack tip, which is attributed to elastic unloading behind the growing crack. On contours remote from the region of crack growth however, the deformation J was approached, i.e the value of J which would be calculated assuming analysis of a stationary crack. In this study however, where the crack is grown through an initially uncracked structure, elastic unloading occurs along the whole length of the crack flank. This may explain why the J values presented in Fig. 10 are low and remain low for domains further away from the crack tip.

CHARACTERISATION OF THE CRACK TIP FIELDS

We next examine the ability of the modified J values to characterise the intensity of the crack tip stress fields given in Fig. 4. For a material with the constitutive law given in eq. 3, Hutchinson [8], and Rice and Rosengren [9], showed that the intensity of the crack tip stress field under small scale yielding is described by

$$\frac{\sigma_{ij}}{\sigma_0} = \left(\frac{J}{\alpha \varepsilon_0 \sigma_0 I_n r} \right)^{\frac{1}{n+1}} \tilde{\sigma}_{ij}^{HRR} \tag{5}$$

where I_n is a dimensionless constant which depends on n, $\tilde{\sigma}_{ij}^{HRR}$ is an angular function and α is a material constant which is 1 for the material under investigation. This is designated as the *HRR* field.

Figure 11 shows that the *HRR* distribution is in good agreement with the normal stress distribution obtained from the simultaneous crack analysis, except very close to the crack tip ($r/(J/\sigma_0) < 1$). Over the physically relevant zone $1 < r/(J/\sigma_0) < 5$, where a small strain deformation assumption is valid, the agreement between the finite-element distribution and the *HRR* field is good. It is noted that a similar analysis performed in [5], which used a focused mesh at the crack tip, showed much better agreement in the region $r/(J/\sigma_0) < 1$. Thus the poor agreement in the region $r/(J/\sigma_0) < 1$ shown in Fig. 11 may be due to mesh design.

The result in Fig. 11 supports the physical validity of the J value calculated by eq. 1 as a crack tip stress intensity parameter from the simultaneous crack analysis. On the other hand, the J values obtained from the 'progressive crack analysis' are

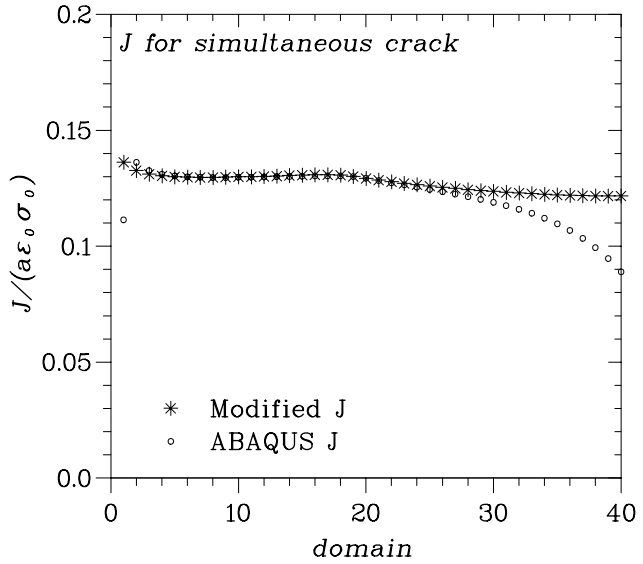

Figure 9. J vs. DOMAIN FOR THE SIMULTANEOUS CRACK, FOR $n = 10$ AND PLANE STRAIN

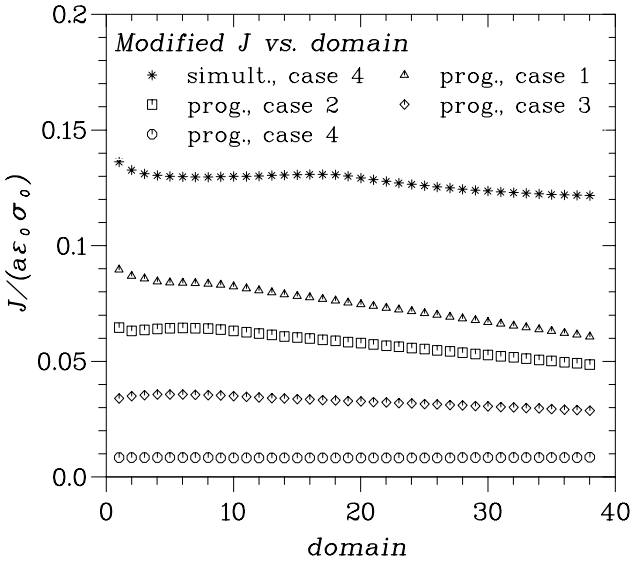

Figure 10. COMPARISON OF J vs. DOMAIN FOR THE SIMULTANEOUS AND PROGRESSIVE CRACKS, FOR $n = 10$ AND PLANE STRAIN

strongly mesh dependent, thus care should be taken in the use of J values obtained from such analyses.

The crack tip plastic zone of the introduced simultaneous crack is found to be small, which suggests that small scale yielding conditions should hold—note that the maximum plastic strain in the uncracked geometry at $x = 0.2w$ (at the location of the introduced crack tip) is 0.3% for the plane strain case, so plasticity due to the initial mechanical deformation of the uncracked geometry is limited. Accordingly, the modified J should be in close agreement with the elastic value of J for the residual stress.

The elastic J has been calculated by carrying out a linear elastic finite-element analysis in which the uncracked residual stress is applied to the crack face, following the superposition principle [10]. Figure 12 shows the comparison between the elastic J and the modified J for the simultaneous crack, from which it may be seen that excellent agreement was obtained. This provides further support of the physical validity of the modified J as a stress intensity characterising parameter for a simultaneous crack.

On the other hand, J for the progressive crack has been shown to be strongly mesh dependent (Fig. 11) and thus its application as a crack tip characterising parameter may be questionable.

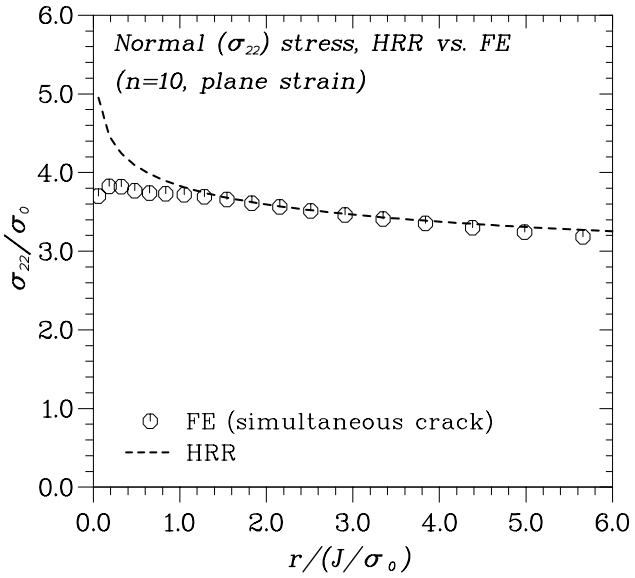

Figure 11. COMPARISON OF THE CRACK TIP STRESS FIELD FOR THE SIMULTANEOUS CRACK WITH THE HRR FIELD, FOR $n = 10$ AND PLANE STRAIN

DISCUSSION

A finite-element investigation has been performed to examine the effect of simultaneous versus progressive crack formation in a residual stress field on the crack tip fields, the crack face displacements and the J-integral. It is shown that the crack tip stress fields for the progressive and simultaneous cracks are similar. The modified J value for the simultaneous crack has been shown to be valid as a stress intensity parameter, whereas the J value for a progressive crack has been shown to be mesh dependent,

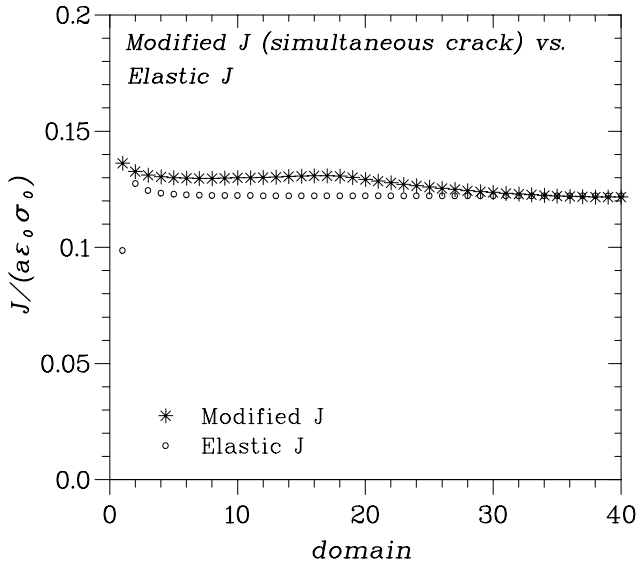

Figure 12. COMPARISON OF MODIFIED J WITH ELASTIC J FOR THE SIMULTANEOUS CRACK, FOR $n = 10$ AND PLANE STRAIN

appearing to approach zero with increasing mesh refinement behind the crack tip. However, since the crack tip stress fields are similar for the simultaneous and progressive crack analyses, this study suggests that J for the simultaneous crack can be used to provide a reasonably accurate and conservative prediction of the stress fields for a progressive crack.

In this work we have shown that the crack face displacements for progressive and simultaneous cracks are similar for both plane strain and plane stress analyses, with the predicted displacements for the simultaneous crack analysis higher than those from a progressive crack analysis (consistent with [4]). Thus a conservative estimate of crack opening displacement would be obtained from a simultaneous crack analysis.

The analysis has been carried out for a range of mesh sizes. For a typical crack length of 2 cm the mesh resolution ranges from 2 μm (Case 4) to 80 μm (Case 1). The results from the simultaneous crack analysis have been found to be relatively mesh insensitive. However, the results for the progressive crack analysis show some mesh dependency, particularly in the J value obtained. The finest mesh used here (Case 4) is considered to provide the converged solution for a continuously growing progressive crack in a residual stress field. The results for the coarser mesh designs could be associated with discontinuous crack growth, with the mesh size associated with a microstructural length, e.g. the grain size. In the latter case, it may be appropriate to carry out a progressive crack analysis with the mesh design based on this physical length scale. Alternatively, if there is uncertainty about the appropriate mesh size, the results from a simultaneous crack analysis can be used. This produces results which are weakly mesh sensitive and leads to conservative (upper-bound) predictions of crack tip stress and strain and crack opening displacement, with an associated path independent J value, which characterises the amplitude of the crack tip stress fields.

CONCLUSIONS

A two dimensional finite-element investigation has been performed to examine the effect of simultaneous vs. progressive crack formation in a residual stress field. The modified J definition for a simultaneous crack has been shown to be physically valid as a stress intensity parameter, though for a progressive crack, J is found to be mesh dependent and should therefore be treated with caution. Since however the crack tip stress fields for progressive and simultaneous crack analyses are similar, this suggests that J for a simultaneous crack can be used to provide a reasonable prediction of the crack tip stresses for a progressive crack.

REFERENCES

[1] British Energy, 2006. *R6 Revision 4: Assessment of the Integrity of Structures containing Defects*.

[2] Rice, J. *et. al.*., 1980. "Elastic-plastic analysis of growing cracks". In *Fracture Mechanics, ASTM STP 700*, G. Halford and J. Gallagher, Eds. American Society for Testing and Materials, Philadelphia, pp. 189–221.

[3] Nilsson, F., 1992. "Numerical investigation of J characterization of growing crack tips". *Nucl. Engng. Des.,* **133**, pp. 457–463.

[4] Sherry, A., Quinta da Fonseca, J., Goldthorpe, M. R., and Taylor, K., 2006. "Measurement and modelling of residual stress effects on cracks". *Fatigue Fract. Engng. Mater. Struct.,* **30**, pp. 243–257.

[5] Lei, Y., O'Dowd, N., and Webster, G., 2000. "Fracture mechanics analysis of a crack in a residual stress field". *Int. J. Fracture,* **106**, pp. 195–216.

[6] Lei, Y., 2005. "J-integral evaluation for cases involving non-proportional stressing". *Eng. Fract. Mech.,* **72**, pp. 577–596.

[7] Hibbitt, Karlsson & Sorensen, I., 2006. *ABAQUS version 6.6*.

[8] Hutchinson, J., 1968. "Singular behaviour at end of tensile crack in hardening material". *J. Mech. Phys. Solids,* **16**, pp. 13–31.

[9] Rice, J., and Rosengren, G., 1968. "Plane strain deformation near crack tip in power-law hardening material". *J. Mech. Phys. Solids,* **16**, pp. 1–12.

[10] Anderson, T., 2005. *Fracture mechanics—Fundamentals and Applications*, third ed. CRC Press.